

# Continuous-time Predator-Prey-Like Systems of Non Linear Ordinary Differential Equations Linking Mosquito-Breeding Site Density to Community Action Under Temperature Effects

Gideon A Ngwa

University of Buea

Miranda Ijang Teboh-Ewungkem (✉ [ewungkems@gmail.com](mailto:ewungkems@gmail.com))

Lehigh University <https://orcid.org/0000-0002-0765-4969>

James A Njongwe

University of Buea

---

## Research Article

**Keywords:** Mosquito breeding site, Precipitation and Temperature, Human Consciousness, Non- Linear Least Squares, Mathematical Modelling, Indicator function

**Posted Date:** March 8th, 2021

**DOI:** <https://doi.org/10.21203/rs.3.rs-173946/v1>

**License:** © ⓘ This work is licensed under a Creative Commons Attribution 4.0 International License.

[Read Full License](#)

---

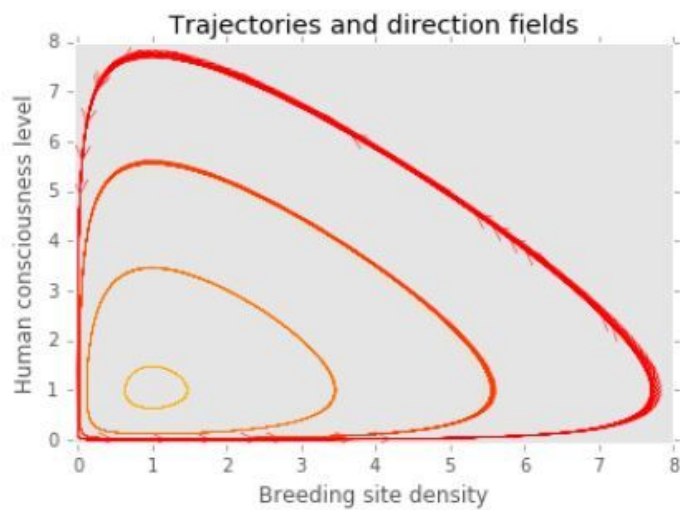
# Abstract

A system of two first order nonlinear ordinary differential equations is used to model and theoretically investigate the dynamics of the formation of mosquito breeding sites in a uniform environment. The model captures the dynamic interplay between community action, climatic factors and the availability of mosquito breeding sites by interpreting the possible pathways and environmental processes leading to the formation of these breeding sites. The developed model is analysed using standard methods in nonlinear dynamical systems' theory. Our results show that it is possible to attempt the problem of the dynamics of formation of breeding sites by taking into consideration the level of human consciousness as measured through human response to community action. Different feedback response functions are used to excite the breeding site removal and community action. For the case where the response functionals are both constants, we identify an indicator function whose size can indicate whether in the long run, community action can lead to the removal and elimination of breeding sites near human habitats. Using a predictor-corrector procedure that fits real climatic data to a continuous periodic function, we demonstrate how climatic variables can be included in the model and how models for the time variation of temperature and precipitation in a given area can be constructed just by appropriately choosing the parameters of a sinusoidal function and then correcting the output using nonlinear least squares analysis. Numerical simulation results are used to complement our analytical results.

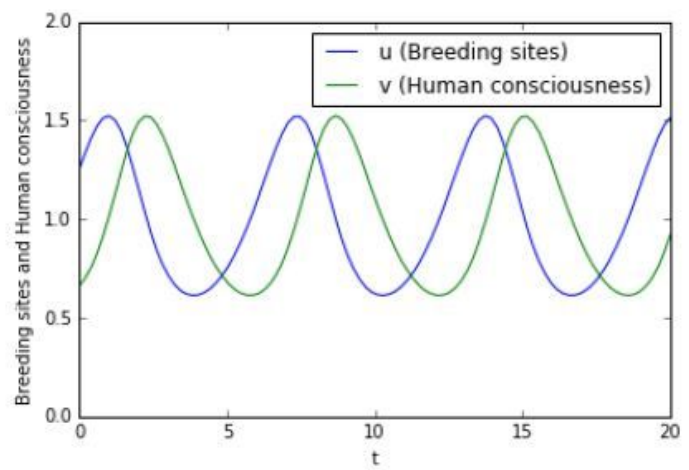
# Full Text

Due to technical limitations, full-text HTML conversion of this manuscript could not be completed. However, the latest manuscript can be downloaded and [accessed as a PDF](#).

# Figures



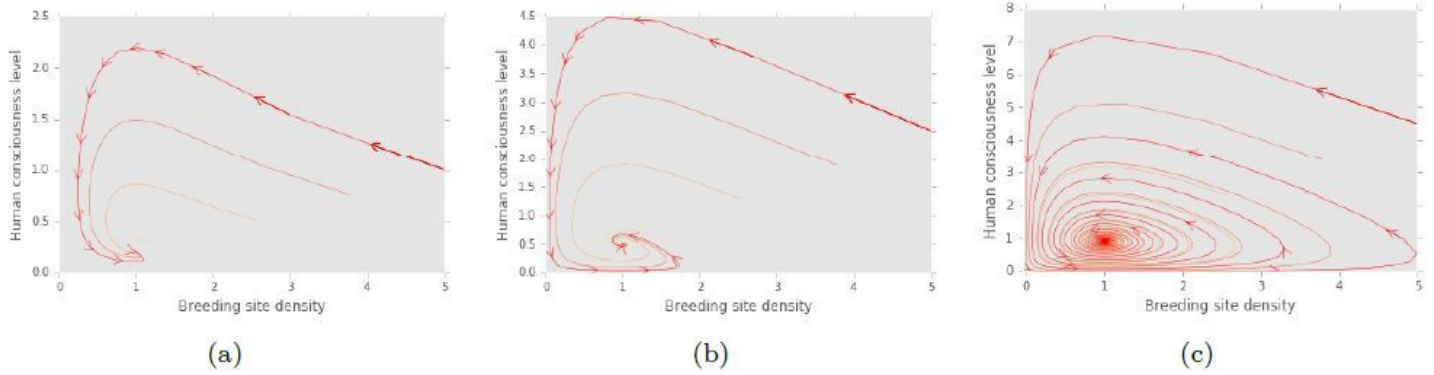
(a)



(b)

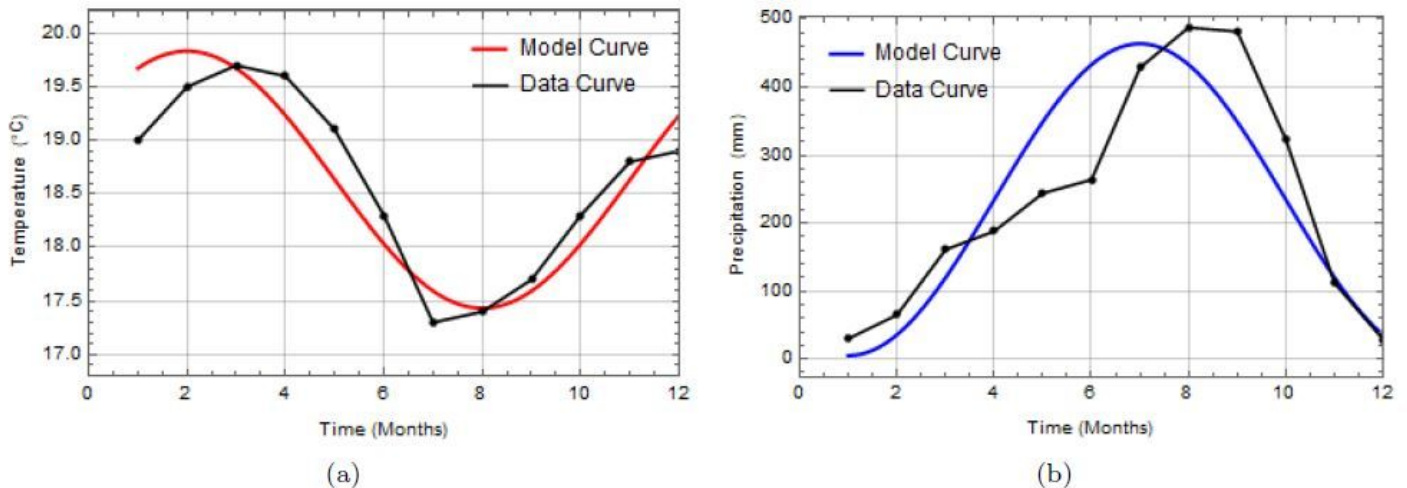
**Figure 1**

Illustration of the output of system (1)-(2) for the case where  $f$  and  $g$  are both monotone increasing and  $K_b = \cdot$ . The system exhibits closed trajectories about the non-zero equilibrium point, shown for different values of the initial condition, while the origin is a saddle point. For the selected parameters, these are expected profiles agreeing with the results from a predator prey model with mass action contact [20, 18, 28]. The solutions show periodic behaviour in time with fixed amplitude and period. The important parameters that determine the period of the oscillations are the linear growth rate of the breeding sites and the rate of waning of human consciousness.



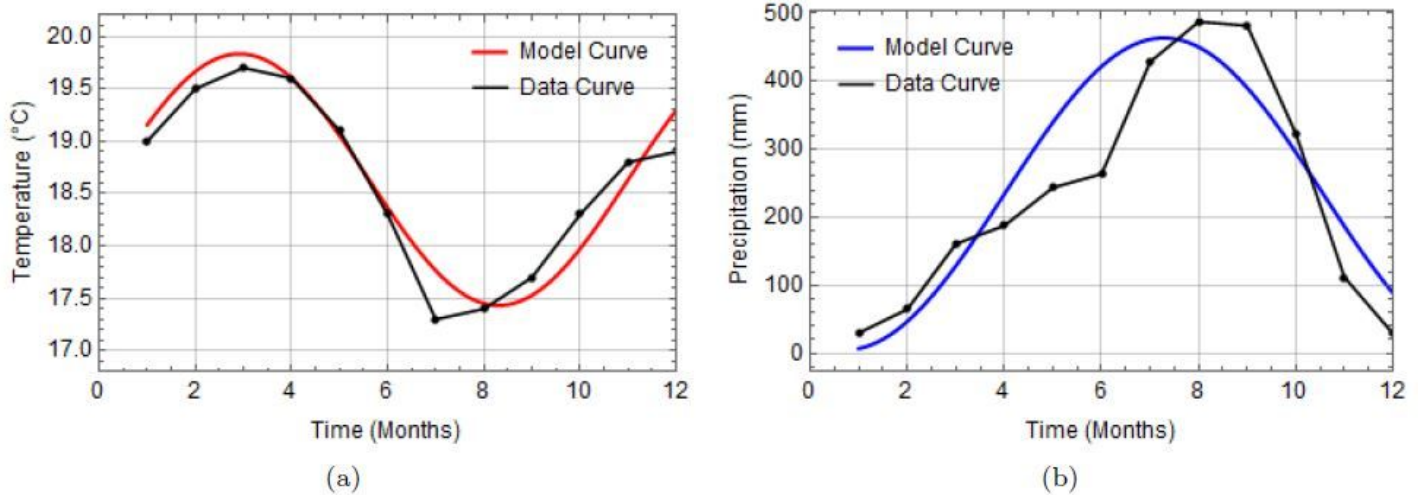
**Figure 2**

Illustration of the output of system (1)-(2) for the case where  $f$  and  $g$  are both monotone increasing and  $K_b < \cdot$ . The system exhibits stable spiral trajectories about the non-zero equilibrium point while the origin is a saddle point. The solutions show periodic behaviour but with ever decreasing amplitude of oscillation, converging to a stable stationary solution. The period of the oscillations depend on the linear growth rate of the breeding sites as well as the rate of waning of human consciousness. (a)  $\xi = 1, \sigma = 1.25$ , (b)  $\xi = 1, \sigma = 2.0$ , (c)  $\xi = 1, \sigma = 10$ .



**Figure 3**

Comparing the profile curves for the temperature and precipitation fitted functions (red and blue curves, respectively) with the actual data curve (black dotted curves) for the locality of Buea, Cameroon, over a period of 12 months, where the actual data is shown in Table 2. Figure (a) compares the temperature profile with the data profile, while Figure (b) compares the precipitation profile with the data. The fitting process of Dangbe et al. [11] gives a reasonable approximation to the temperature and precipitation data points. We can therefore use the continuous approximation given by the formulas for  $T(t)$  and  $P(t)$  defined by (37) and (38), respectively, in our modelling framework. However, as can be seen in this figure, the predictions (37) and (38) when compared with the real data, shows clearly that there is an appreciable error in the fitted data.



**Figure 4**

Comparing the curves for the corrected profiles for the temperature and precipitation fitted functions (red and blue curves, respectively) with the data curve (black dotted curves) for the locality Buea, Cameroon, over a period of 12 months. The actual data is shown in Table 2. Figure (a) compares the corrected temperature fitted profile with the data profile, while Figure (b) compares the corrected precipitation profile with the data. The fitted data shown in Figure 3 by the predictions (37) and (38) when compared with the real data, shows clearly that there was an appreciable error in the fitted data. Nonlinear least squares was used to improve the approximation and it gave the values  $k = k_b + \varepsilon = 0.583212$  and  $\omega = \omega_b + \varepsilon = 0.4787$  which should be used in formulas (37) and (38).

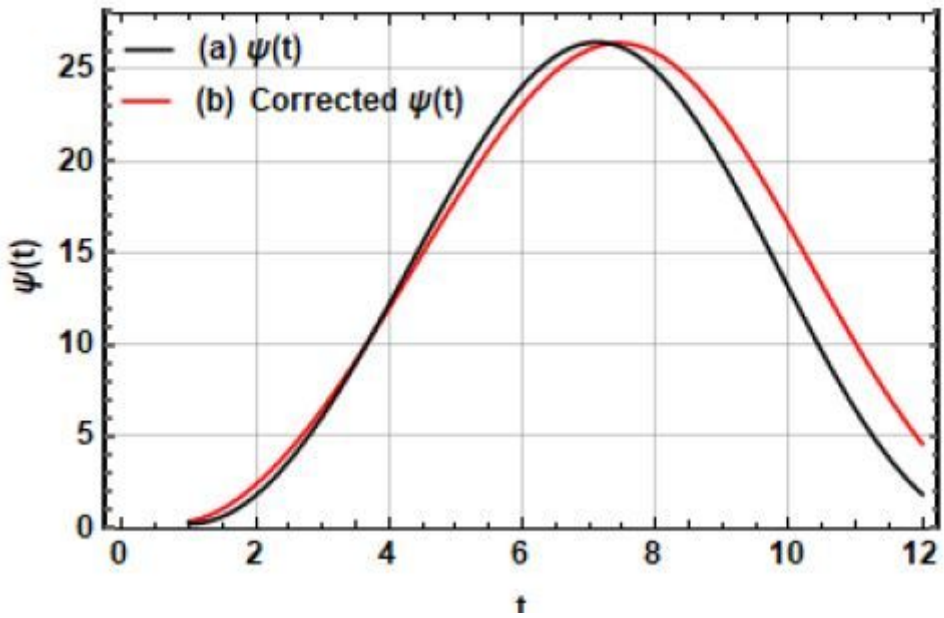


**Figure 5**

Graphs of  $\psi(t)$  obtained using the approximations formulas for  $T(t)$  and  $P(t)$ . Graph (a) corresponds to the plot  $\psi(t)$  obtained using the initial temperature and precipitation approximation functions  $T(t) = 18.6 + 1.2 \sin [0.5236(t - 11)]$  and  $P(t) = 234.6 + 229.5 \sin [0.5236(t - 4)]$ , respectively, while Graph (b) corresponds to the plot of  $\psi(t)$  obtained using the corrected temperature and precipitation approximation functions  $T(t) = 18.6 + 1.2 \sin [0.583212(t - 11)]$  and  $P(t) = 234.6 + 229.5 \sin [0.478703(t - 4)]$ . Clearly the corrected graph adjusts for the peak months.

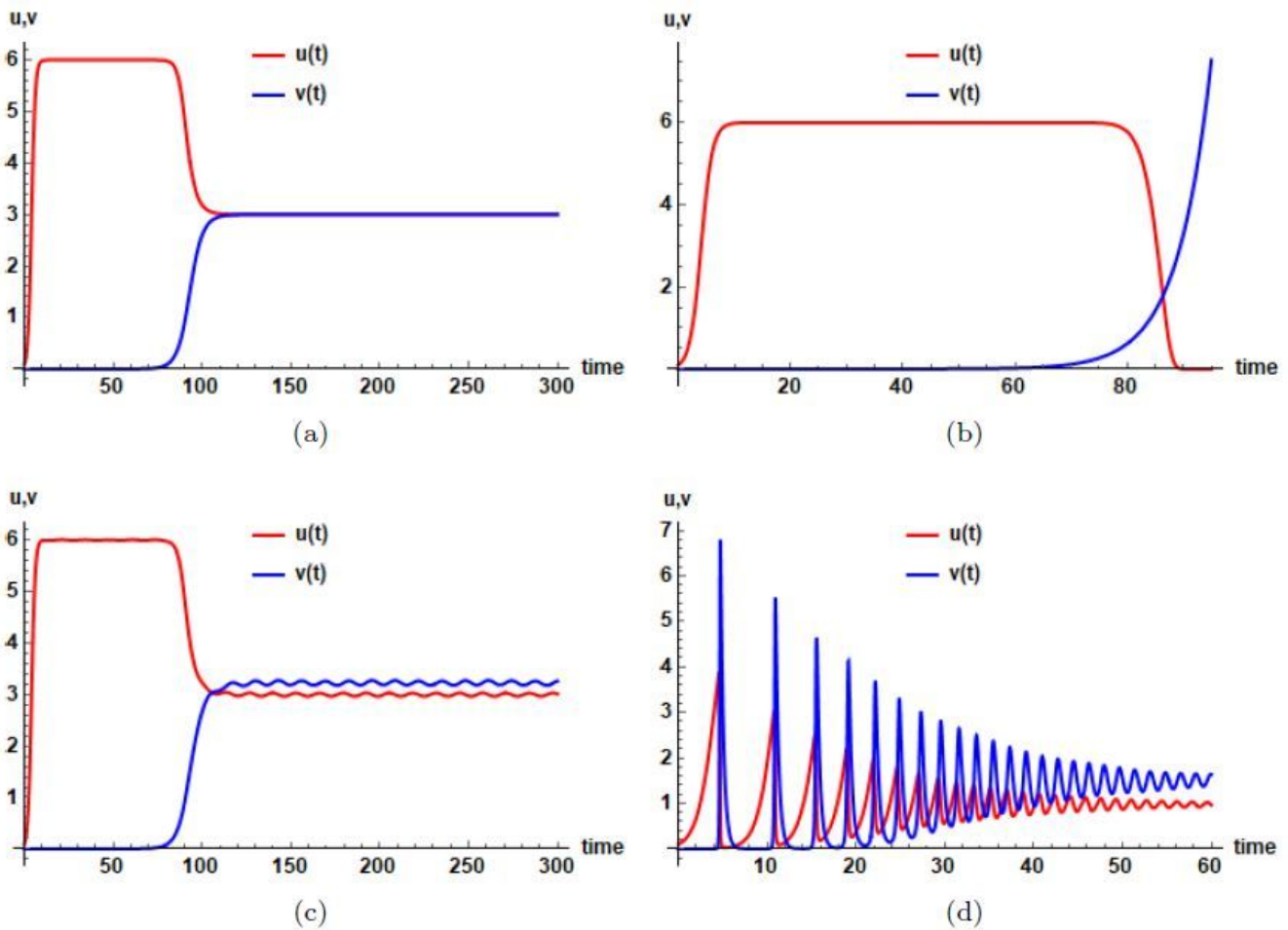


**Figure 6**

Illustrations of the behaviour of the solution with different forms of the functions  $\tilde{f}$  and  $\tilde{g}$  in system (51)-(52) where  $\tilde{f}$  and  $\tilde{g}$  are scaled from (47). As the density of breeding sites rises it triggers a corresponding rise in human consciousness which eventually brings down the density of breeding sites to the steady state levels as in (a) or removes the breeding sites completely as in (b). When climatic factors are allowed to come into play, the level of consciousness rises and stays above the density of breeding sites showing sustained community action potential as in (c) and (d). In each of graphs (a)-(d),  $\alpha = 5$ ,  $\beta = 6$ , and  $v = 3$ , all fixed. The parameters  $\delta$ ,  $r_0$  and  $k_0$ , as well as  $n$ ,  $m$ ,  $p$ ,  $q$ , the sensitivity indices of the response functions  $\tilde{f}$  and  $\tilde{g}$ , with respect to changes in the density of breeding site and level of consciousness, are varied. Graph (a) shows convergence of the long time solution to a steady state for  $n = m = p = q = 2$ ,  $\delta = 10$  and  $r_0 = k_0 = 0$ . In (b),  $r_0 = k_0 = 0$  as in (a), but  $n = 4$ ,  $m = 2$ ,  $p = q = 0.9$  and  $\delta = 19.9$ , and the level of consciousness leads to elimination of breeding sites. Both (a) and (b) showcase the dynamics in the absence of climatic effects. In (c), the same parameters as in (a) are used except  $r_0 = 10^{-3}$ ,  $k_0 = 10^{-4}$  and the dynamics approaches a limit cycle with much smaller amplitudes. In (d),  $n = 4$ ,  $m = 2$ ,  $p = 3$ ,  $q = 2$ ,  $r_0 = 0.001$ ,  $k_0 = 0.005$  and  $\delta = 19$ . In graphs (c) and (d), climatic factors are

in effect, with precipitation and temperature regarded as perturbation from the system without climatic factors. The scaled initial data is such that  $u(0) = 10^{-1}$ ,  $v(0) = 10^{-5}$ .

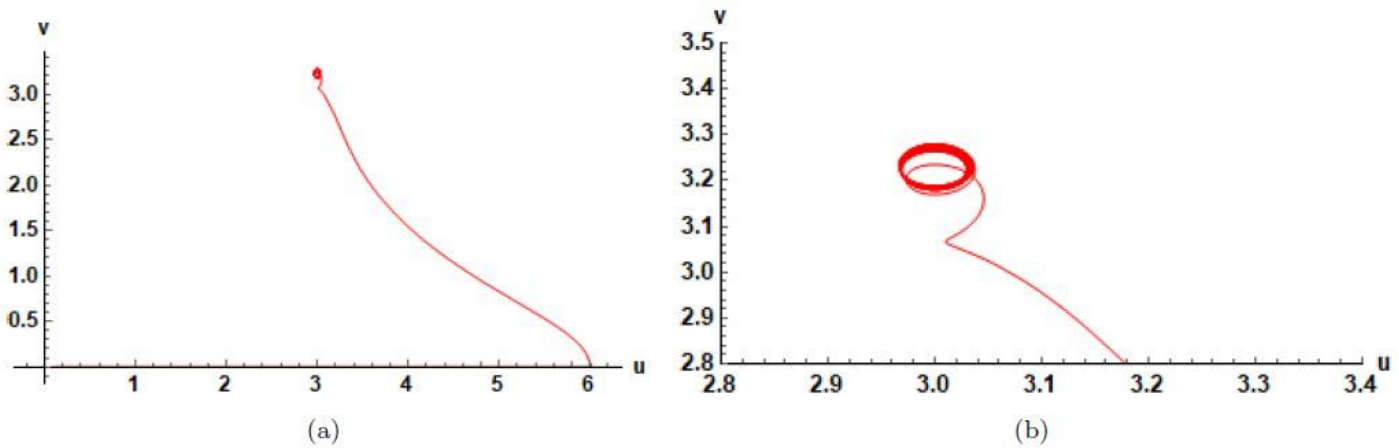


**Figure 7**

Illustration of the transient and parametric behaviour of the solution curves for Figure 6(c) where  $n = m = p = q = 2$ ,  $\delta = 10$  and  $r_0 = 10^{-3}$ ,  $k_0 = 10^{-4}$ . The amplitudes of the oscillations are very small in this case. Graph (a) shows the plots over the entire range of  $u$  and  $v$  while graph (b) shows the regions close to the limit cycle.

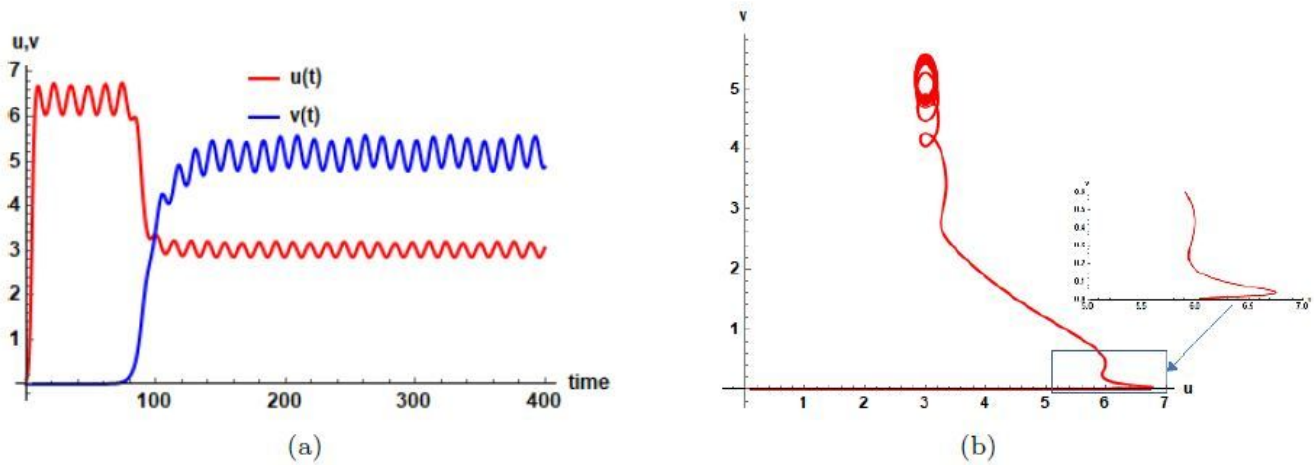


**Figure 8**

Illustration of the transient and parametric behaviour of the solution for  $n = m = p = q = 2$ ,  $\alpha = 5$ ,  $\beta = 1$ ,  $\delta = 10$ ,  $\nu = 3$ ,  $r_0 = 0.001$  and  $k_0 = 0.005$ . As the density of breeding sites rises to 9.69 a cyclical pattern, it eventually triggers a corresponding rise in human consciousness. Eventually, the level of consciousness reaches a size that leads to action towards breeding site reduction. But the level of consciousness cycles in a pattern, not strong enough to eliminate the breeding site. The breeding site density also cycles in its own pattern with the two, the level of consciousness and breeding site density, eventually entering into a limit cycle as shown in graph (b). Here, climatic factors are in effect, and as in Figure 6, precipitation and

temperature are regarded as perturbation from the system without climatic factors, with the scaled initial data such that  $u(0) = 10^{-1}$ ,  $v(0) = 10^{-5}$ .